The Numerical Investigation on Hydrodynamic Performance of Twisted Rudder during Self-propulsion

Cong Liu[*], Jianhua Wang，Decheng Wan[‡]

State Key Laboratory of Ocean Engineering, School of Naval Architecture, Ocean and Civil Engineering, Shanghai Jiao Tong University, Collaborative Innovation Center for Advanced Ship and Deep-Sea Exploration, Shanghai 200240, China

[*]Presenting author: maximusliu@sjtu.edu.cn

[‡]Corresponding author: dcwan@sjtu.edu.cn

http://dcwan.sjtu.edu.cn

Abstract

In the present work, Comparison of Energy Efficiency Performance between a twisted rudder and an ordinary spade rudder is conducted during self-propulsion. The energy-saving mechanism of twisted rudder is revealed by numerical simulation. This study is carried out using our solver naoe-FOAM-SJTU. The governing equations are unsteady Reynolds-Averaged Navier-Stokes (URANS) equations discretized by finite volume method (FVM). Overset technique is employed to handle the propeller rotation. To prepare for self-propulsion simulations, the open water curves of propeller and bare hull resistance are previously obtained by our solver. These two results show good agreement with experimental data. Based on that, the self-propulsion simulations to estimate the speed performance with twisted rudder and spade rudder are carried out. The results show that twisted rudder boosted hull efficiency by 2.4% through reducing the thrust deduction fraction and raising the hull efficiency. The delivered power is also decreased by 3.9% in the model scale comparing with ordinary rudder. The flow field around the propeller- rudder system shows that twisted rudder efficiently retrieves y-direction momentum to x-direction and improves the propulsive performance.

Keywords: twisted rudder; self-propulsion; overset grids; naoe-FOAM-SJTU solver

Introduction

In the context of global warming, the International Maritime Organization (IMO) issued mandatory standard which requires all ships larger than 400 gross tonnage reducing Energy Efficiency Design Index (EEDI) by up to 30% after 2025. To achieve this goal, more efficient rudders which can increase the propulsion are helpful. As we all known, the propeller produces thrust by rotating around its shaft which inevitably induces swirl energy loss. Aiming to retrieve this residual energy, several scholars designed a twisted rudder which can transfer part of rotation energy to propulsion. For example, a benchmark case, Duisburg Test Case(DTC), was designed to equip with a twisted rudder[1]. The energy-saving mechanism of twisted rudder can be explained as follow. The propeller creates a pair of opposing wake flows around the propeller shaft center. Generally, for a clockwise-rotating propeller, wake flow above the shaft centre turns toward port side, then the twisted rudder's leading edge is designed to twist port and vice versa below the shaft. Since the angle of attack of the twisted rudder is smaller than that of the horn-type rudder, the twisted rudder profile can decrease drag and lift to some extent [2]. Twisted rudder can also transfer the cross-stream velocity to stream wise more efficiently and improve the propulsive efficiency. A twisted rudder with a bulb may have 4% less fuel consumption[3]. Sun et al.[4] studied the hydrodynamic characteristics of twisted rudder through both experimental and numerical method. The

energy-saving mechanism and cavitation performance were analyzed without taking the hull body in to account. Kim et al.[2] reported that a Z-twisted rudder, which has a Z-shaped leading edge, with and without a fin may reduce the fuel consumption by 2.35% and 2.95% via self-propulsion model tests. In the paper, CFD method was also used to analyze the fluid characteristics of the twisted rudder. but the effect of free surface was neglected. They assumed that the twisted rudder has no influence on propeller' RPS, so the self-propulsion condition was simplified by fixing the model and keeping propeller's rotational speed at constant value.

In this paper, taking the rudder's effect on PRS into account, the author tries to estimate the speed performance for a ship with twisted and ordinary rudders during self-propulsion. Several validations and preparations need to be done before the self-propulsion simulations. To estimate the wake fraction during the self-propulsion, the open water curves of propeller is firstly calculated by our solver. Then to estimate the friction deduction, the resistance of towed ship without propeller is obtained. Based on that，the propulsion factors for two kinds of rudders are obtained from the self-propulsion simulations using our solver, naoe-FOAM-SJTU. In our solver, a six-degree-of-freedom (6DoF) module coupled with overset grid technique[5] is utilized to simulate the rotation of propeller and predict the motions of ship. This solver has been successfully applied in the region of predicting the ship maneuverability. For example, Wang et al.[6] used our solver to simulate ship self-propulsion with moving propellers and rudders. Furthermore, Wang et al.[7] carried out turning circle simulation by our solver.A twisted rudder and an ordinary spade rudder are compared. The predicted thrust deduction and hull efficiency are validated with the experimental data[1].

This paper is organized as follows: In the first section, a brief introduction of the numerical methods is given. Then an open-water curves and resistance of bare hull are predicted. Next, the simulations of the self-propulsion are following. Then the differences in propulsion factors and hydrodynamic characteristics between two kinds of rudder are analyzed. Finally, a summary of the paper is presented.

Numerical method

Governing Equations

The incompressible Navier-Stokes equations are the governing equations, which can be written as:

$$\nabla \cdot \boldsymbol{U} = \boldsymbol{0} \tag{1}$$

$$\frac{\partial \rho \boldsymbol{U}}{\partial t} + \nabla \cdot \left(\rho\left(\boldsymbol{U} - \boldsymbol{U_g}\right)\boldsymbol{U}\right) = -\nabla p_d - \boldsymbol{g} \cdot \boldsymbol{x}\nabla\rho + \nabla \cdot \left(\mu_{eff}\nabla \boldsymbol{U}\right) \tag{2}$$

where U is fluid velocity field and $\boldsymbol{U}_g$ is the grid velocity; $p_d = p - \rho \boldsymbol{g} \cdot \boldsymbol{x}$ is the dynamic pressure, obtained by subtracting the hydrostatic component from the total pressure; ρ is the mixture density; $\boldsymbol{g}$ is the gravity acceleration; $\mu_{eff} = \rho(\nu + \nu_t)$is effective dynamic viscosity, in which ν and ν_t are kinetic and eddy viscosity, respectively, and ν_t is obtained from turbulence model.

Overset Grid Technique

Overset grid is a grid system composed of multiple blocks of overlapping structured or unstructured grids. In a full overset grid system, a complex geometry is decomposed into a

system of geometrically simple overlapping grids. Boundary information is exchanged between these grids via interpolation of the fluid variables. Through this way overset grid method removes the restrictions of the mesh topology among different objects and allows grids move independently within the computational domain, and can be used to handle with large amplitude motion in the field of ship and ocean engineering. The most critical technique in the overset is the accomplishment of information exchange between grids. Based on the numerical methods from OpenFOAM including the cell-centered scheme and unstructured grids, SUGGAR++ is utilized to generate the domain connectivity information (DCI) for the overset grid interpolation in our solver naoe-FOAM-SJTU. Through this way, the solver can handle with arbitrary motion in the simulation.

Computations and Results

Open water propeller test

Before we move on to the self-propulsion test, the open water curve is predicted using overset grid technique. This step has two purposes. First, it is used to validate the basic dynamic overset grids strategy and implementation by comparison with experimental data. Second, the open water propeller performance is needed for a full CFD prediction of the self-propulsion factors.

The propeller is a fixed-pitch five-bladed propeller with right rotation. This propeller is equipped on Duisburg Test Case(DTC). Table 1 shows its main particulars: propeller diameter D_P ,pitch ratio at 0.7 of propeller radius $P_{0.7}/D_P$, disc ratio A_e/A_0 , chord length $c_{0.7}$ at 0.7 of propeller radius, effective skew angle of propeller blades θ_{eff} and non-dimensional hub diameter d_h/D_P. Figure 1 shows it geometric feature.

Table 1 Propeller parameters

	Model scale	Full Scale
D_P [m]	0.15	8.911
$P_{0.7}/D_P$ [m]	0.959	0.959
A_e/A_0 [m]	0.8	0.8
$c_{0.7}$ [mm]	0.054	3.208
θ_{eff} [°]	31.97	31.97
d_h/D_P [-]	0.176	0.176

Figure 1 view of the propeller

An earth-fixed frame of reference is used where the propeller is moving with constant rotational speeds and towed with a small acceleration to cover a wide range of advance velocity in a single run. The computations use the single-run procedure described in Xing et al.[10] The grid system is composed of two parts: overset grid used to follow the rotation of propeller and background grid used to accommodate the far-field boundary conditions (see Figure 2). The grids interpolated by Suggar++ are illustrated in Fig. 3. The two grids are separately generated by SnappyHexMesh, an automatic mesh-generation utility provided by OpenFOAM. The sizes of these grids are listed in Table 2. The time step is set to $\Delta t = 2 \times 10^{-4} s$.The RPS is fixed at 13.5 n / s and thrust and torque coefficients K_T and K_Q, and efficiency η_0 for each advance coefficient are obtained from the thrust and torque as showed in Figure 4,. In the single-run procedure, the propeller is accelerated from J=0 to1 in 5 s.

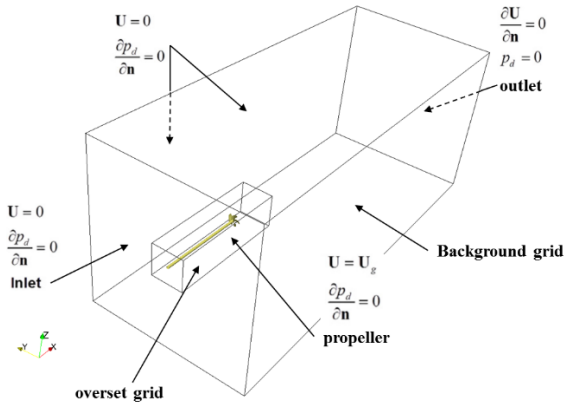

Figure 2 Design of the over set grid system and boundary conditions for the propeller.

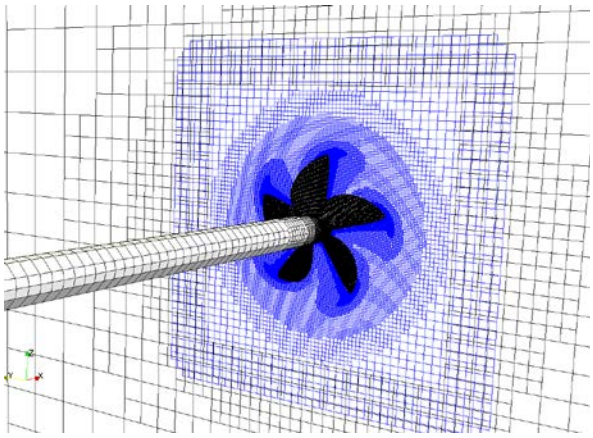

Figure 3 Grids used for open water computations overset

Table 2 mesh size for open water propeller

	background	Overset	Total
Cells number	116,963	3,060,690	3,177,653

Figure 4 shows that the overset technique predicts the curves quite well and results have a good agreement with experimental data, except for J > 0.8 where η_0 is over estimated. Figure 5 illustrates the vortical structure using isosurfaces of Q=200, the second invariant of the velocity gradient tensor. The vortices shed from three position: tips, trailing edges and hub. These results indicate that the overset technique is capable of predicting the open-water curves and will be used to estimate the effective wake friction in the condition of self-propulsion.

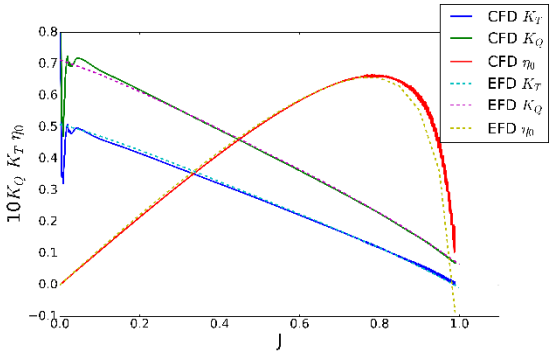

Figure 4 Open water curves for experiments(dash lines),single-run(solid lines)procedures

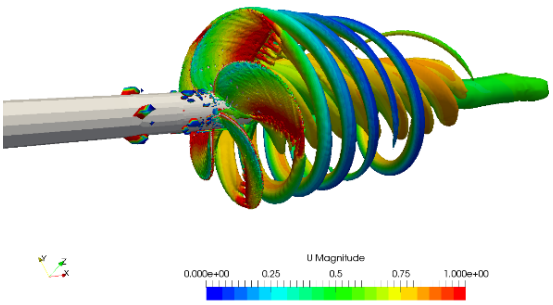

Figure 5 Iso-surfaces of Q=200 at J=0.61

Towed DTC without propeller

Before self-propulsion, the hull resistance should be calculated previously for two reason. In the case of self-propulsion, the hull resistance R_T needs to be obtained, which will be used to estimate the friction deduction and the convergence result of resistance calculation will be used to initialize the initial condition of the self-propulsion to achieve faster convergence.

The model chosen to calculate is Duisburg Test Case(DTC) and the experiments data of hull resistance and self-propulsion can be found in el Moctar[1]. Its characteristics are shown in Figure 6, and its principal particulars are listed in Table 3: Length between perpendiculars L_{pp} , waterline breadth B_{wl} , draught midships T_m, trim angle θ, volume displacement V, block coefficient C_B , wetted surface under rest waterline without appendages S_w .DTC design features a twisted rudder with Costa bulb and a NACA 0018 base profile (see Figure 6, bottom).

Table 3 Main dimensions of DTC in design loading condition

		Model scale	Full scale
L_{pp}	[m]	5.976	355
B_{wl}	[m]	0.859	51
T_m	[m]	0.244	14.5
θ	[]	0	0
V	[m3]	0.827	173467
C_B	[-]	0.661	0.661
S_w	[m2]	6.243	22032

Figure 6 View of Duisburg Test Case hull(top), rudder (bottom))

The speed is 1.668 m/s, corresponding to *Fr=0.218* and the time step is $1 \times 10^{-3}s$. The results compared with experimental data can be find in Table 4 ,including resistance R_T, and its non-dimensional coefficient $C_T = R_T / (0.5 / \rho S_w v^2)$, frictional resistance R_F and its non-dimensional coefficient $C_F = R_F / (0.5 \rho S_w v^2)$, and non-dimensional wave resistance coefficient $C_W = R_W / (0.5 \rho S_w v^2)$. For experimental data, the frictional resistance coefficient C_F was calculated according to ITTC 1957 as $C_F = 0.075 / (log_{10} Re - 2.0)^2$ and the wave resistance coefficient was estimated as $C_W = C_T - (1 + k) C_F$,where form factor $k = 0.094$.

Table 4 Resistance coefficients for DTC bare hull with twisted rudder

	$R_{T\,[N]}$	$R_{F[N]}$	$C_T \times 10^{-3}$	$C_F \times 10^{-3}$	$C_W \times 10^{-4}$
Experimental data	31.83	26.431	3.67	3.047	3.36
Present work	30.19	25.38	3.48	2.928	2.821
Error	-4.39%	-4.14%	-5.46%	-4.06%	-5.66%

The comparisons in Table 4 show quite well agreement between CFD and experimental data. The hull resistance coefficients are underestimated by CFD in the range 4.06%-5.66%. This results show that our solver has the ability to precisely predict the hull resistance. The total hull resistance coefficients C_T obtained by CFD will be used to calculate the friction deduction.

Self-propelled DTC with twisted and spade rudder.

For self-propulsion, DTC is equipped with a directly rotating propeller, which provides the thrust for the ship to advance. The self-propulsion is performed at ship point by adding a friction deduction force of the form

$$F_D = 0.5\rho_M S_{WM} V_M^2 (C_{TM} - C_T) \quad (5)$$

where index M denotes model scale. C_{TM} =3.48×10^{-3} obtained from previous CFD results. The total resistance coefficient C_T is defined at the corresponding temperature. Then F_D=13.41 N

Following Carrica et al.[7], aproportional-integral(PI) controller is employed to adjust the rotational speed of the propeller to achieve the desired ship speed. The instantaneous RPS of the propeller, n, is obtained as $n = Pe + I\int edt$,where P and I are proportional and integral constants, respectively, and e is the error between target ship speed and instantaneous speed, $e = U_{target} - U_{ship}$ .Using the PI controller, we will get the final balance condition at certain RPS of propeller where $T = R_T - F_D$ and U_{ship}=U_{target} .This procedure resembles the self-propulsion experiment using continental method.

The assessment of the rudder performance can be conduct in two ways. The first way is to conduct the assessment at constant propeller's rotational speed n. This method presumes that there is a negligible change in n due to difference in the twisted rudder's design parameter. Through this way, it is convenience to compare the flow fields and the rudders which the resistance of rudder-propeller system is smaller would be considered to have a better rudder performance. In Kim's work, the calculation part was conducted in this indirect way.

But the comparison would best be taken at the self-propulsion point. Through the PI controller, it is possible to directly compare the influence of rudder shape on the propulsive performance at self-propulsion point. For the ships equipped with twisted or ordinary spade rudder， use the PI controller to achieve the target speed and obtain the values of RPS of propeller, propeller thrust and hull efficiency respectively. Then the influence of rudder on propeller performance can be obtain by comparing these values. The merit of this method is that the propeller performance can be compared in an intuitive and practical way. In Kim's work, the experiment part was conducted in this direct way.

In present work, numerical calculation is use to achieve the comparison both at the self-propulsion point and at constant propeller's rotational speed. In computation, the origin of the Earth coordinate system is located at the intersection of the waterline and the ship's bow with the longitudinal x-axis pointing fore to aft, the transversal y-axis pointing from port to starboard, and the vertical z-axis pointing upward. The profile of two kind of rudder is showed in Figure 7 and Figure 8.The spade rudder is obtained by extending the twisted rudder's root profile along the 1/4 chord line and keeping the chord length invariant. The layout of grids system and boundary conditions for self-propulsion calculation can be found in Figure 9.

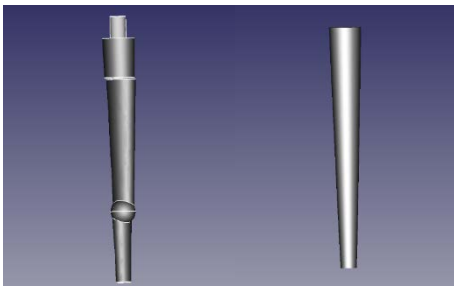

Figure 7 front view of rudders(left: twisted rudder, right: spade rudder)

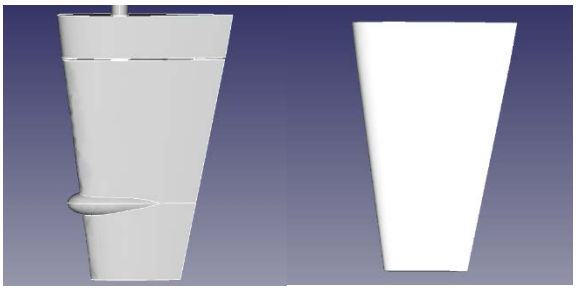

Figure 8 side view of rudders(left: twisted rudder, right: spade rudder)

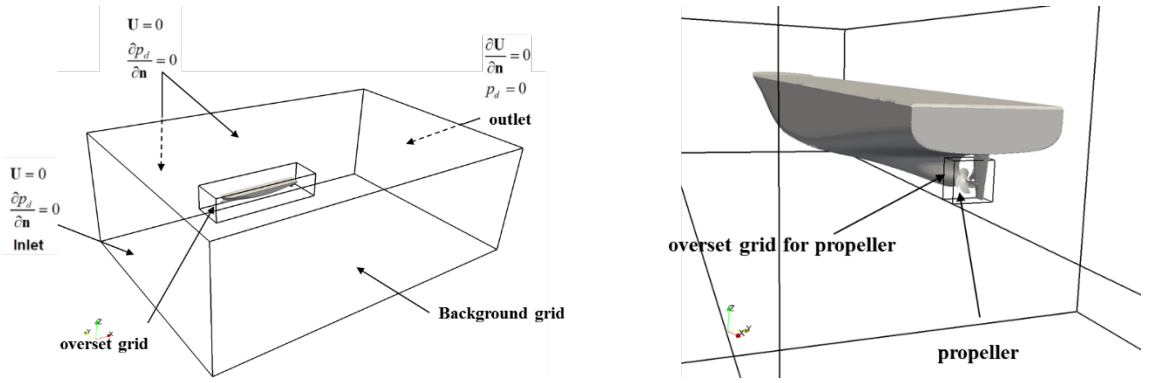

Figure 9 Overset grid system and boundary conditions for self-propelled DTC (left :global view , right: close view)

The time histories of RPS and thrust forces are shown in Figure 10 and Figure 11 respectively. The computation was run for 9s of model scale time. After 6s, the RPS converged to the self-propulsion point.

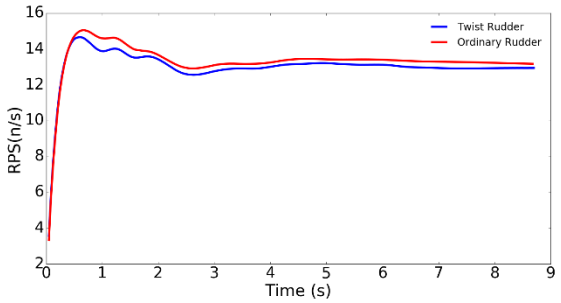

Figure 10 Time history of RPS(blue line represents twisted rudder and red line represents ordinary rudder)

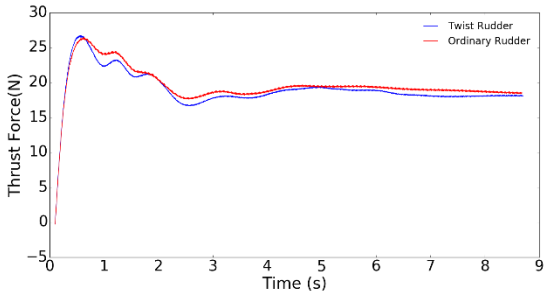

Figure 11 Time history of Thrust forces (blue line represents twisted rudder and red line represents ordinary rudder)

The experimental data of Self-propelled DTC equipped with twisted rudder can be found in el Moctar[1].Table 5 shows the experimental data compared with present work results

Table 5 Resistance coefficients and propulsion factors for self-propelled DTC.

		Present	Experiment data	Error
Resistance Coefficience	C_T	3.48E-03	3.67E-03	5.1%

Thrust deduction	1-t	0.957	0.91	5.2%
Effecticve wake coefficient	1-w	0.762	0.725	-5.1%
Hull efficiency	η	1.256	1.26	0.1%

The RPS of propeller equipped with twisted rudder or ordinary spade rudder at self-propulsion points are 12.8n/s and 13.1n/s, respectively. Due to the twisted rudder, the propeller's RPS decreases by 2.84%. The torque of twisted rudder and ordinary spade are $0.355\,N\cdot M$ and 0.361 $N\cdot M$ corresponding to delivered power P_D are 28.55 W and 29.71 W, respectively. P_D for twisted rudder decreased by 3.9%. Table 6 shows the difference of propulsion factors for two type rudders.

Table 6 Propulsion factors for self-propelled DTC with different rudders

	Thrust coefficient K_T	Thrust Deduction t	Wake fraction ω	Hull efficiency η_H
Twisted rudder	0.202	0.043	0.238	1.256
Spade rudder	0.198	0.058	0.232	1.23
Difference	1.9%	-25.8%	2.59%	2.4%

The main role of the twisted rudder is to lower the t to raise the hull efficiency (η_H). The thrust deduction drop (25.8%) is because the required thrust forces reduces. The rudder causes the wake fraction, ω, to rise 1.8%. The hull efficiency (η_H) rises (2.4%) from the reduced t and increased ω.

To demonstrate the energy-saving mechanisms of twisted rudder, the self- propulsion simulation is conducted in a more restrained way, namely, the ship speed and RPS of propeller are the same for the ships equipped with two type rudder. As we argued before, twisted rudder profiles transferring the cross-stream velocity to stream wise retrieve part of the rotation energy to propulsion. So it is natural to compare the distribution of velocity components around the propeller-rudder system.

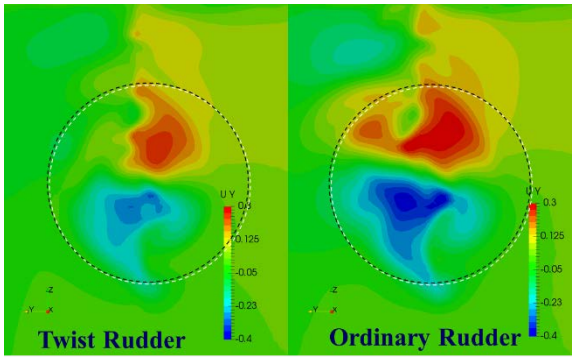

Figure 12 y-direction velocity components contours downstream of the rudder.

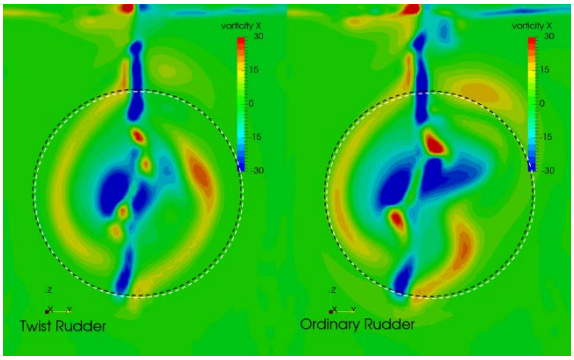

Figure 13 Axial vorticity contours downstream of the rudder

Figure 12 shows the y-direction velocity components contours downstream of the two kinds of rudders. It is evident that the twisted rudder reduces the magnitude of y-direction velocity. Meanwhile the Axial vorticity is also reduced(see Figure 13). Figure 14 and Figure 15 show the y-direction velocity on the horizontal surfaces below and above the shaft centre, respectively. For the twisted rudder，the y-direction velocity magnitude is smaller than the ordinary rudder in front of the region of leading edge. Considering the y-direction velocity has

no contribution to propulsion, the less the y –direction velocity is, the more efficient the propeller is.

Figure 16 shows the x-direction velocity on horizontal surface above the shaft centre. It is obvious that the x-velocity distribution near the twisted rudder are more straight forward than the ordinary rudder. All these velocity components contours indicate that the twisted rudder more efficiently transfers y-direction momentum to x-direction and improves the propulsive performance.

Figure 17 compares the dynamic pressure distribution on the propellers pressure sides for two kinds of rudders. In the case of the twisted rudder, the maximal pressure distribution is more widely found on the pressure side than ordinary rudder which indicates that the propeller produces more thrust force with the twisted rudder at the same RPS.

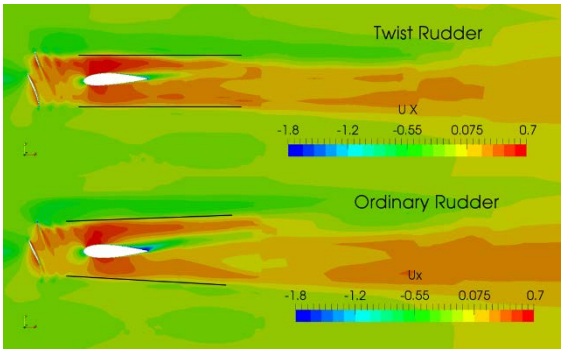

Figure 14 x-direction velocity components contours on horizontal cross-sections above the shaft centre

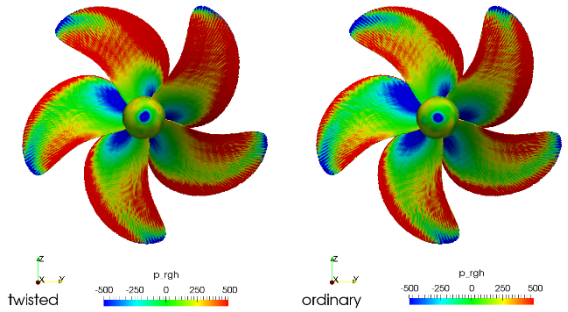

Figure 15 dynamic pressure contours on the pressure sides

Conclusions

In this paper, the energy-saving mechanism of twisted rudder is discussed and studied by numerical methods. All simulations are performed by our solver, naoe-FOAM-SJTU, developed under the framework of the open source OpenFOAM packages. Overset technique is applied to handle with propeller rotation and ship motions. The propeller open-water curves are obtained using the single run methodology, achieving good agreement with experimental data. Computations of the towed bare hull DTC are performed as needed to obtain self-propulsion factors. Resistance coefficients are compared against experimental data showing good results. Two kinds of rudders speed performance is predicted at the self-propulsion point. The results show that twisted rudder boosts hull efficiency by 2.4% through reducing the thrust deduction fraction and raising the hull efficiency. The results of delivered power is decreased by 3.9% in the model scale. The flow fields around the propeller- rudder system show that twisted rudder efficiently transfers y-direction momentum to x-direction and improves the propulsive performance.

Acknowledgements

This work is supported by the National Natural Science Foundation of China (51379125, 51490675, 11432009, 51579145), Chang Jiang Scholars Program (T2014099), Shanghai Excellent Academic Leaders Program (17XD1402300), Program for Professor of Special Appointment (Eastern Scholar) at Shanghai Institutions of Higher Learning (2013022), Innovative Special Project of Numerical Tank of Ministry of Industry and Information

Technology of China (2016-23/09) and Lloyd's Register Foundation for doctoral student, to which the authors are most grateful.

References

[1] el Moctar, O., Shigunov, V., and Zorn, T. (2012) Duisburg Test Case: Post-panamax container ship for benchmarking, *Ship Technology Research* **59**(3), 50–64.

[2] Kim, J.-H., Choi, J.-E., Choi, B.-J., and Chung, S.-H. (2014) Twisted rudder for reducing fuel-oil consumption, *International Journal of Naval Architecture and Ocean Engineering* **6**(3), 715–722.

[3] Liu, J., and Hekkenberg, R. (2017) Sixty years of research on ship rudders: effects of design choices on rudder performance, *Ships and Offshore Structures* **12**(4), 495–512.

[4] Sun, Y., Su, Y., and Hu, H. (2015) Experimental Study and Numerical Simulation on Hydrodynamic Performance of a Twisted Rudder, *Marine Technology Society Journal* **49**(5), 58–69.

[5] Shen, Z., Wan, D., and Carrica, P.M. (2015) Dynamic overset grids in OpenFOAM with application to KCS self-propulsion and maneuvering, *Ocean Engineering* **108**, 287–306.

[6] Wang, J., Zhao, W., and Wan, D. (2016) Self-propulsion Simulation of ONR Tumblehome Using Dynamic Overset Grid Method, *Proceding of 7th International Conference on Computational Methods*, Berkeley, USA, No. ID 1499-5539-1-PB.

[7] Wang, J., Zhao, W., and Wan, D. (2016) Free maneuvering simulation of ONR tumblehome using overset grid method in naoe-FOAM-SJTU [C], *31st Symposium on Naval Hydrodynamics*, Monterey, CA, USA.

[8] Rusche, H. (2003) Computational fluid dynamics of dispersed two-phase flows at high phase fractions, Ph.D. Imperial College London (University of London).

[9] Berberović, E., Hinsberg, N.P. van, Jakirlić, S., Roisman, I.V., and Tropea, C. (2009) Drop impact onto a liquid layer of finite thickness: Dynamics of the cavity evolution, *Physical Review E* **79**(3), 036306.

[10] Xing, T., Carrica, P., and Stern, F. (2008) Computational Towing Tank Procedures for Single Run Curves of Resistance and Propulsion, *Journal of Fluids Engineering* **130**(10), 101102.

[11] Carrica, P.M., Castro, A.M., and Stern, F. (2010) Self-propulsion computations using a speed controller and a discretized propeller with dynamic overset grids, *Journal of Marine Science and Technology* **15**(4), 316–330.